LECTURE NOTES IN COMPUTATIONAL SCIENCE AND ENGINEERING 112

Bülent Karasözen · Murat Manguoğlu
Münevver Tezer-Sezgin · Serdar Göktepe
Ömür Uğur *Editors*

Numerical Mathematics and Advanced Applications ENUMATH 2015

Springer

Lecture Notes in Computational Science and Engineering 112

Editors:

More information about this series at http://www.springer.com/series/3527

Bülent Karasözen • Murat Manguoğlu •
Münevver Tezer-Sezgin • Serdar Göktepe •
Ömür Uğur
Editors

Numerical Mathematics and Advanced Applications ENUMATH 2015

Springer

Editors
Bülent Karasözen
Mathematics & Applied Mathematics
Middle East Technical University
Ankara, Turkey

Murat Manguoğlu
Department of Computer Engineering
Institute of Applied Mathematics
Ankara, Turkey

Münevver Tezer-Sezgin
Department of Mathematics
Middle East Technical University
Ankara, Turkey

Serdar Göktepe
Civil Engineering & Applied Mathematics
Middle East Technical University
Ankara, Turkey

Ömür Uğur
Institute of Applied Mathematics
Middle East Technical University
Ankara, Turkey

ISSN 1439-7358 ISSN 2197-7100 (electronic)
Lecture Notes in Computational Science and Engineering
ISBN 978-3-319-39927-0 ISBN 978-3-319-39929-4 (eBook)
DOI 10.1007/978-3-319-39929-4

Library of Congress Control Number: 2016956100

Mathematics Subject Classification (2010): 65XX, 74XX, 76XX, 78XX

Printed on acid-free paper

This Springer imprint is published by Springer Nature
The registered company is Springer International Publishing AG Switzerland

Preface

The European Conference on Numerical Mathematics and Advanced Applications (ENUMATH) is a series of conferences held every 2 years to provide a forum for discussion on recent aspects of numerical mathematics and scientific and industrial applications. The previous ENUMATH meetings took place in Paris (1995), Heidelberg (1997), Jyvaskyla (1999), Ischia (2001), Prague (2003), Santiago de Compostela (2005), Graz (2007), Uppsala (2009), Leicester (2011), and Lausanne (2013).

This book contains a selection of invited and contributed lectures of the ENUMATH 2015 organized by the Institute of Applied Mathematics, Middle East Technical University, Ankara, Turkey, September 14–18, 2015. It gives an overview of recent developments in numerical analysis, computational mathematics, and applications by leading experts in the field. The conference attracted around 300 participants from around the world including 11 invited talks by:

- Assyr Abdulle (EPF Lausanne, Switzerland), *Reduced Basis Multiscale Methods*
- Rémi Abgrall (Universität Zürich, Switzerland), *Recent Progress on Non-Oscillatory Finite Element Methods for Convection Dominated Problems*
- Burak Aksoylu (TOBB University of Economics and Technology, Ankara, Turkey), *Incorporating Local Boundary Conditions into Nonlocal Theories*
- Mark Ainsworth (Brown University, Providence, USA), *Multigrid at Scale?*
- Willi Freeden (TU Kaiserslautern, Germany), *Principles in Geomathematically Reflected Numerics and Their Application to Inverse Potential Methods in Geothermal Exploration*
- Des Higham (University of Strathclyde, Glasgow, UK), *Models and Algorithms for Dynamic Networks*
- Yvon Maday (UniversitéĄ Pierre et Marie Curie, Paris, France), *Towards a Fully Scalable Balanced Parareal Method: Application to Neutronics*
- Kaisa Miettinen (University of Jyväskylä, Finland), *Examples of Latest Interactive Method Developments in Multiobjective Optimization*
- Mario Ohlberger (Universität Münster, Germany), *Localized Model Reduction for Multiscale Problems*

- Anders Szepessy (KTH, Stockholm, Sweden), *On Global and Local Error with Application to Adaptivity, Inverse Problems and Modeling Error*
- Eugene E. Tyrtyshnikov (Russian Academy of Sciences, Moscow, Russia), *Tensor Decompositions and Low-Rank Matrices in Mathematics and Applications*

There were 119 minisymposia presentations in 20 sessions, and 89 contributed talks covering a broad spectrum of numerical mathematics. This ENUMATH 2015 proceeding will be useful for a wide range of readers giving them a state-of-the-art overview of advanced techniques, algorithms, and results in numerical mathematics and scientific computing. This book contains a selection of 61 papers by the invited speakers and from the minisymposia as well as the contributed sessions. It is organized in IX parts as follows:

We would like to thank all the participants for their valuable contributions and scientific discussions during the conference and to the minisymposium organizers for helping to shape the core structure of the meeting. The members of the Scientific Committee have helped us tremendously in reviewing the contributions to this proceedings. This conference would not have been possible without all the work and guidance provided by the program committee: Franco Brezzi, Miloslav Feistauer, Roland Glowinski, Gunilla Kreiss, Yuri Kuznetsov, Pekka Neittaanmaki, Jacques Periaux, Alfio Quarteroni, Rolf Rannacher, Endre Süli, and Barbara Wohlmuth. We also thank our sponsors for their generous support: Middle East Technical University, Scientific Human Resources Development Program (ÖYP) of Ministry of Development, Turkish Academy of Sciences, Oxford University Press, and Springer Verlag. We would like to acknowledge the tireless effort of ATAK Tours; Murat Uzunca, who coordinated the edition of this Proceedings; all the staff of the Institute of Applied Mathematics for their tremendous help in organizing this conference; and our students who have helped us in many ways.

This volume is dedicated to the 60th anniversary of Middle East Technical University.

Ankara, Turkey
April 2016

Bülent Karasözen
Murat Manguoğlu
Münevver Tezer-Sezgin
Serdar Göktepe
Ömür Uğur

Contents

Part I
Space Discretization Methods for PDEs

DRBEM Solution of MHD Flow and Electric Potential in a Rectangular Pipe with a Moving Lid

Münevver Tezer-Sezgin and Canan Bozkaya

Abstract We present the dual reciprocity boundary element method (DRBEM) solution of the system of equations which model magnetohydrodynamic (MHD) flow in a pipe with moving lid at low magnetic Reynolds number. The external magnetic field acts in the pipe-axis direction generating the electric potential. The solution is obtained in terms of stream function, vorticity and electric potential in the cross-section of the pipe, and the pipe axis velocity is also computed under a constant pressure gradient. It is found that fluid flow concentrates through the upper right corner forming boundary layers with the effect of moving lid and increased magnetic field intensity. Electric field behavior is changed accordingly with the insulated and conducting portions of the pipe walls. Fluid moves in the pipe-axis direction with an increasing rate of magnitude when Hartmann number increases. The boundary only nature of DRBEM provides the solution at a low computational expense.

1 Introduction

MHD is the study of the interaction of electrically conducting fluids and electromagnetic forces. It has a widespread applications in designing cooling systems with liquid metals, MHD generators, accelerators, nuclear reactors, blood flow measurements, pumps, flow meters and etc. The most widely-known applications such as MHD flow of liquid metals are considered at low magnetic Reynolds number neglecting induced magnetic field in the fluid. The corresponding physical applications are usually MHD flows inside the pipes. When the external magnetic field applies in the pipe-axis direction, due to the interaction with the electrically conducting fluid, the electric potential is generated which can be made use of in MHD generators.

M. Tezer-Sezgin (✉) • C. Bozkaya
Department of Mathematics, Middle East Technical University, 06800, Ankara, Turkey
e-mail: munt@metu.edu.tr; bcanan@metu.edu.tr

B. Karasözen et al. (eds.), *Numerical Mathematics and Advanced Applications ENUMATH 2015*, Lecture Notes in Computational Science and Engineering 112, DOI 10.1007/978-3-319-39929-4_1

The DRBEM is a technique that offers a great advantage to solve MHD flow equations treating all the terms (including nonlinear) other than diffusion as inhomogeneity. The studies carried by BEM and DRBEM for solving the MHD equations in pipes of several cross-sections are given in [1–6]. The externally applied magnetic field in these works is taken parallel to the cross-section plane with different orientations. Han Aydın et al. [7] and Tezer-Sezgin et al. [8] have presented also stabilized FEM and BEM-FEM solutions for MHD flow in ducts and for biomagnetic fluids, respectively. Biomagnetic fluid flow in cavities (ducts) is also studied by Tzirtzilakis [9–11] by using pressure-linked pseudotransient method on a collocated grid and finite volume method with SIMPLE algorithm, respectively.

In this paper, MHD flow in a pipe imposed to an external magnetic field in the direction of the pipe-axis is simulated using DRBEM in the cross-section of the pipe as a two-dimensional problem. The electric potential and pipe-axis velocity are also obtained with DRBEM. The boundary only nature of DRBEM gives efficient solution even by using constant elements with considerably small computational cost compared to other numerical methods.

2 The Physical Problem and Mathematical Formulation

The steady flow of an incompressible, electrically conducting, viscous fluid in a pipe in the presence of an external magnetic field acting in the pipe-axis direction is considered.

The governing dimensionless MHD equations are [12, 13]

$$\frac{1}{N}(\boldsymbol{u}.\nabla)\boldsymbol{u} - \frac{1}{M^2}\nabla^2\boldsymbol{u} + \frac{1}{N}\nabla p = \boldsymbol{B}\times\nabla\phi + \boldsymbol{B}\times(\boldsymbol{B}\times\boldsymbol{u}) \tag{1}$$

$$\nabla.\boldsymbol{u} = 0, \quad \nabla.\boldsymbol{B} = 0, \quad E = -\nabla\phi, \quad \nabla^2\phi = \operatorname{div}(\boldsymbol{u}\times\boldsymbol{B}) \tag{2}$$

where $\boldsymbol{u} = (u_x, u_y, u_z)$, p, $\boldsymbol{B} = (0, 0, B_0)$, ϕ are the fluid velocity, pressure, magnetic field and the electric potential, respectively. M and N are Hartmann and Stuart numbers given by $M = B_0 L\dfrac{\sqrt{\sigma}}{\sqrt{\rho\nu}}$, $N = \sigma B_0^2\dfrac{L}{\rho U_0}$ where σ, ρ, ν are the electrical conductivity, density and kinematic viscosity of the fluid, L and U_0 are the characteristic length and the velocity, and B_0 is the intensity of the applied magnetic field. Induced magnetic field is neglected due to the low magnetic Reynolds number, and $M^2 = N\,Re$, Re being fluid Reynolds number.

Flow is two-dimensional in the cross-section of the pipe (see Fig. 1) giving

$$\frac{\partial u_x}{\partial x} + \frac{\partial u_y}{\partial y} = 0 \tag{3}$$

$$\frac{1}{N}\left(u_x\frac{\partial u_x}{\partial x} + u_y\frac{\partial u_x}{\partial y}\right) - \frac{1}{M^2}\nabla^2 u_x + \frac{1}{N}\frac{\partial p}{\partial x} = -\frac{\partial\phi}{\partial y} - u_x \tag{4}$$

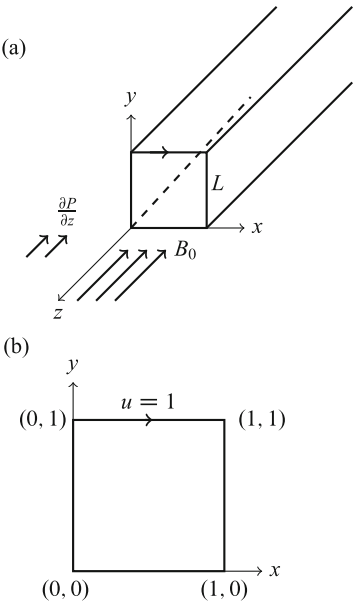

Fig. 1 (**a**) Problem domain and (**b**) cross-section of the pipe

$$\frac{1}{N}\left(u_x\frac{\partial u_y}{\partial x}+u_y\frac{\partial u_y}{\partial y}\right)-\frac{1}{M^2}\nabla^2 u_y+\frac{1}{N}\frac{\partial p}{\partial y}=\frac{\partial \phi}{\partial x}-u_y \tag{5}$$

$$\frac{1}{N}\left(u_x\frac{\partial u_z}{\partial x}+u_y\frac{\partial u_z}{\partial y}\right)-\frac{1}{M^2}\nabla^2 u_z=-\frac{1}{N}\frac{\partial P}{\partial z} \tag{6}$$

where the pressure $P = p(x, y) + P_z(z)$ is divided into the cross-section pressure $p(x, y)$ and, the pipe-axis pressure $P_z(z)$ with constant $\frac{\partial P_z}{\partial z}$.

Introducing stream function and vorticity in two-dimensional cross-section as

$$u_x=\frac{\partial \psi}{\partial y},\quad u_y=-\frac{\partial \psi}{\partial x},\quad w=\frac{\partial u_y}{\partial x}-\frac{\partial u_x}{\partial y}$$

we have

$$\nabla^2\psi=-w \tag{7}$$

$$\nabla^2\phi=w \tag{8}$$

$$\frac{1}{N}\left(u_x\frac{\partial w}{\partial x}+u_y\frac{\partial w}{\partial y}\right)-\frac{1}{M^2}\nabla^2 w=0 \tag{9}$$

$$\frac{1}{N}\left(u_x\frac{\partial u_z}{\partial x}+u_y\frac{\partial u_z}{\partial y}\right)-\frac{1}{M^2}\nabla^2 u_z=-\frac{1}{N}\frac{\partial P_z}{\partial z}\,. \tag{10}$$

On the boundary of the cavity, stream function is a constant due to the known velocity value, electric potential or its normal derivative is zero according to insulated or conducting portions, and the vorticity is not known.

3 DRBEM Application

DRBEM treats all the right hand side terms of Eqs. (7), (8), (9), and (10) as inhomogeneity, and an approximation for this inhomogeneous term as proposed [14] is

$$b \approx \sum_{j=1}^{K+L} \alpha_j f_j = \sum_{j=1}^{K+L} \alpha_j \nabla^2 \hat{u}_j$$

where K and L are the numbers of boundary and interior nodes, α_j are sets of initially unknown coefficients, and the f_j are approximating radial basis functions linked to particular solutions $\hat{u}_j$ with $\nabla^2 \hat{u}_j = f_j$. The radial basis functions f_j are usually chosen as polynomials of distance between the source point (x_i, y_i) and the field point (x_j, y_j) as $r_{ij} = \sqrt{(x_i - x_j)^2 + (y_i - y_j)^2}$.

DRBEM transforms differential equations defined in a domain Ω to integral equations on the boundary $\partial\Omega$. For this, differential equation is multiplied by the fundamental solution $u^* = -\ln(r)/2\pi$ of Laplace equation and integrated over the domain. Using Divergence theorem for the Laplacian terms on both sides of the equation, domain integrals are transformed to boundary integrals.

For the discretization of the boundary, constant elements are used to obtain DRBEM matrix-vector form for Eqs. (7), (8), (9), and (10) as

$$(H\psi - G\frac{\partial \psi}{\partial n}) = (H\hat{U} - G\hat{Q})F^{-1}\{-w\} \tag{11}$$

$$(H\phi - G\frac{\partial \phi}{\partial n}) = (H\hat{U} - G\hat{Q})F^{-1}\{w\} \tag{12}$$

$$\frac{N}{M^2}\left(Hw - G\frac{\partial w}{\partial n}\right) = (H\hat{U} - G\hat{Q})F^{-1}\left\{u_x\frac{\partial w}{\partial x} + u_y\frac{\partial w}{\partial y}\right\} \tag{13}$$

$$\frac{N}{M^2}\left(Hu_z - G\frac{\partial u_z}{\partial n}\right) = (H\hat{U} - G\hat{Q})F^{-1}\left\{u_x\frac{\partial u_z}{\partial x} + u_y\frac{\partial u_z}{\partial y} + \frac{\partial P_z}{\partial z}\right\}. \tag{14}$$

Equations (11), (12), (13), and (14) are solved iteratively with an initial vorticity. With the computed ψ, the velocity components $u_x = \dfrac{\partial \psi}{\partial y}$ and $u_y = -\dfrac{\partial \psi}{\partial x}$ are

computed using coordinate matrix F with entries $f_{ij} = 1 + r_{ij}$ as

$$u_x = \frac{\partial F}{\partial y} F^{-1}\psi, \quad u_y = -\frac{\partial F}{\partial x} F^{-1}\psi$$

and substituted in the vorticity and pipe-axis velocity equations. All the other space derivatives are computed using F matrix.

4 Numerical Results

The problem geometry is the lid-driven cavity $\Omega = [0,1] \times [0,1]$ which is the cross-section of the pipe where the top layer is moving in the positive x-direction. External magnetic field $\boldsymbol{B} = (0, 0, B_0)$ applies perpendicular to Ω and generates electric potential interacting with the electrically conducting fluid in the pipe. Fluid moves with the movement of the lid and the constant pressure gradient $\frac{\partial P_z}{\partial z} = -8000$ opposite to pipe-axis direction. $K = 120$ and $L = 900$ constant boundary elements and interior nodes, respectively, are taken to simulate the flow and electric potential. Solution is obtained, by using linear radial basis functions $f_{ij} = 1 + r_{ij}$ in the F matrix, for increasing values of Hartmann number M, keeping Stuart number $N = 16$ fixed. Effect of M on the pipe axis-velocity u_z is also visualized.

In Fig. 2 we present streamlines, equivorticity and equipotential lines in the case of electrically conducting pipe wall ($\phi = 0$) for Hartmann number values $M = 20$, 100, 150, 200 which correspond to Reynolds numbers $Re = 25$, 625, 1406, 2500, respectively, since $M^2 = N\,Re$. It is observed that an increase in the strength of the applied magnetic field (increase in M) causes the primary vortex of streamlines to move through the center of the cavity. Recirculations appear at the lower corners and finally at the left upper corner with further increase in M and the movement of the lid to the right. Vorticity moves away from the cavity center towards the walls indicating strong vorticity gradients. The fluid begins to rotate with a constant angular velocity and it flows creating boundary layers near the top and right walls through the upper right corner. Electric potential has the same pattern and magnitudes of streamlines since $\nabla^2\phi = w$, $\nabla^2\psi = -w$ and both ψ and ϕ are zero for this case on the cavity walls.

Figure 3 shows the increase in the magnitude of the pipe-axis velocity u_z with an increase in M when $\frac{\partial P_z}{\partial z} = -8000$. The damping in the magnitude of u_z is seen close to the moving lid as M increases ($M = 20, 50, 100, 150$).

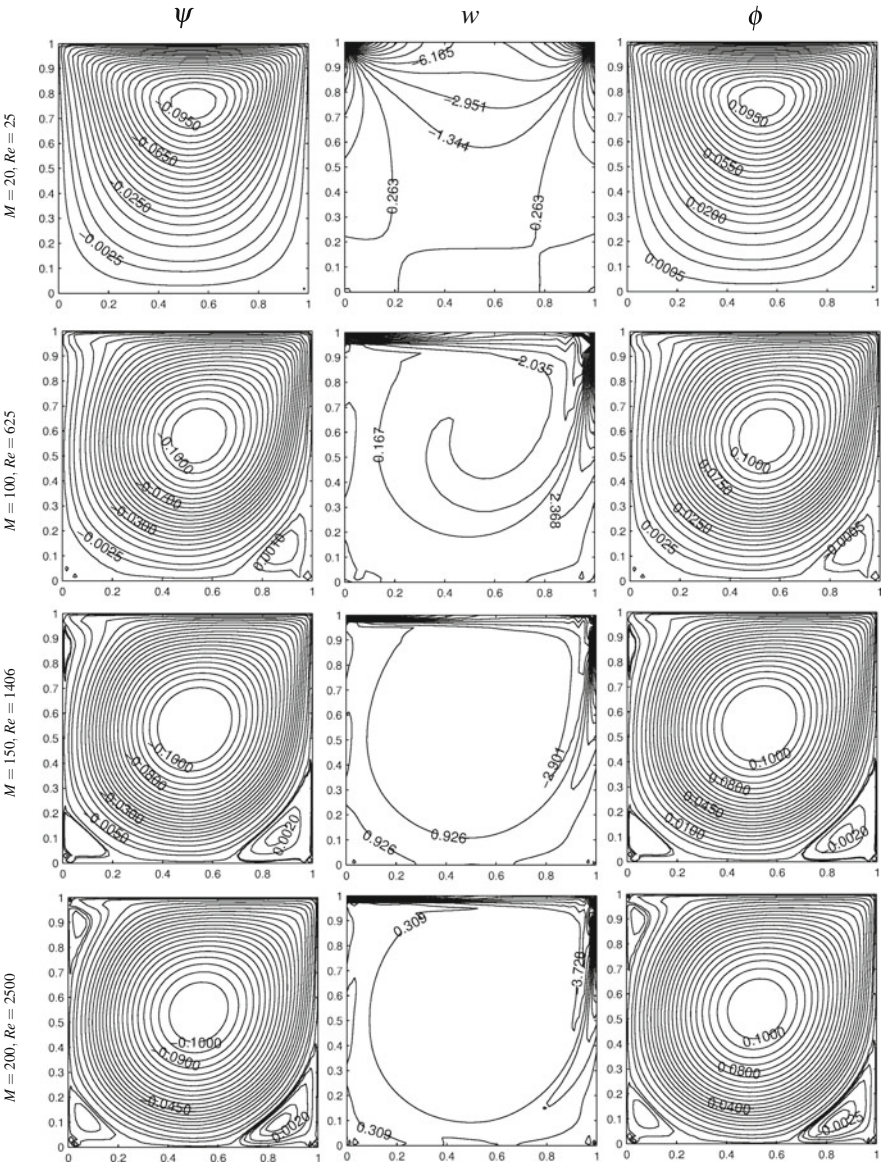

Fig. 2 Effect of Hartmann number on ψ, w and ϕ when $\phi = 0$ on the walls

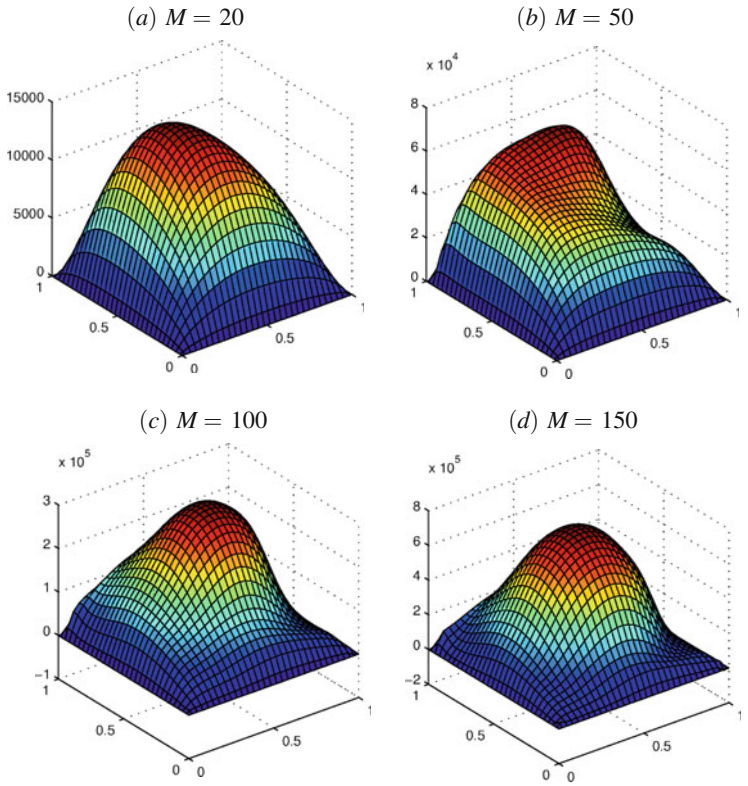

Fig. 3 Pipe-axis velocity u_z when $\phi = 0$ on the walls: (**a**) $M = 20$, (**b**) $M = 50$, (**c**) $M = 100$, (**d**) $M = 150$

When the cavity walls are partly insulated and partly conducting, electric potential leaves the behavior of the flow and obeys boundary conditions on the walls for small values of M. It is seen from Fig. 4 that insulated vertical walls force the potential to touch these walls and then both the increased magnetic intensity and moving lid cause it to regain the flow behavior. On the other hand, insulated top and bottom walls give completely different pattern for the flow as traveling electric waves from the bottom to the top. Increasing Hartmann number does not change this behavior much but tends to concentrate through the upper right corner.

5 Conclusion

The MHD flow in a pipe generates electric potential when the external magnetic field applies in the pipe-axis direction. Increasing Hartmann number shows the same behavior on the flow as if increasing Reynolds number. This is the development of

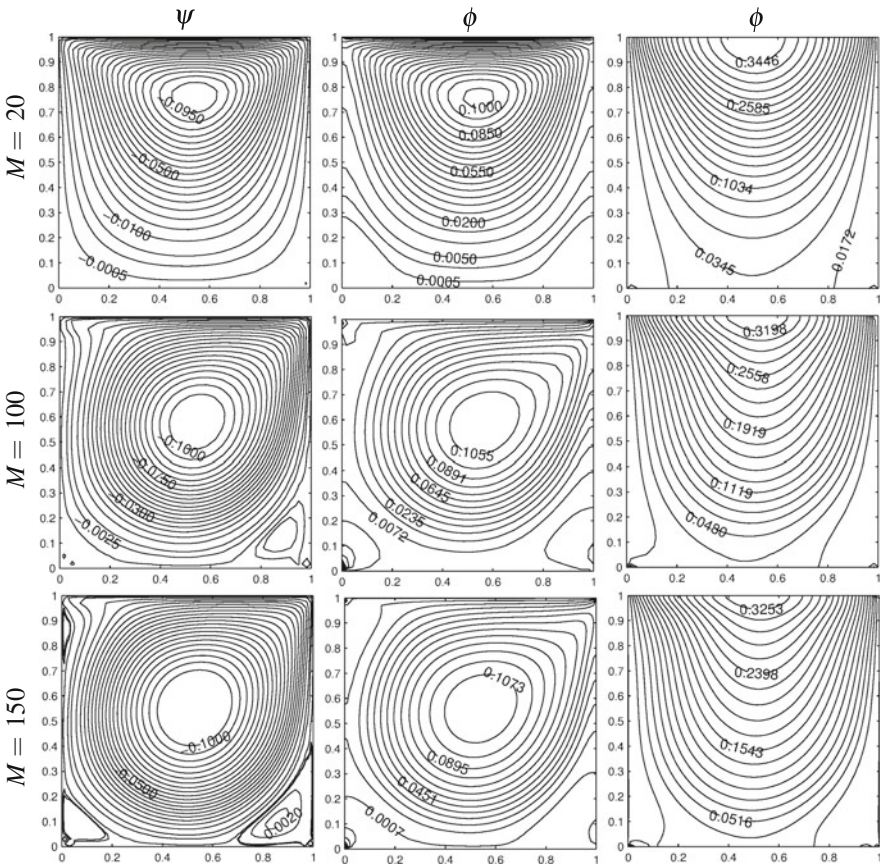

Fig. 4 Effect of Hartmann number on ψ and ϕ when $\frac{\partial \phi}{\partial n}|_{x=0,1} = 0$ (*middle*) and $\frac{\partial \phi}{\partial n}|_{y=0,1} = 0$ (*right*)

secondary flows near the lower corners and third flow close to upper right corner. This behavior is reached for much smaller *Re* values with the effect of applied magnetic field. Vorticity develops gradients on the moving lid and the right wall. Electric potential has the same behavior of the flow only when pipe walls are conducting. Pipe-axis velocity increases in magnitude with an increase in *M*.

References

1. C. Bozkaya, M. Tezer-Sezgin, Fundamental solution for coupled magnetohydrodynamic flow equations. J. Comput. Appl. Math. **203**, 125–144 (2007)
2. C. Bozkaya, M. Tezer-Sezgin, Boundary element method solution of magnetohydrodynamic flow in a rectangular duct with conducting walls parallel to applied magnetic field. Comput. Mech. **41**, 769–775 (2008)

3. M. Tezer-Sezgin, S. Han-Aydın, Solution of MHD flow problems using the boundary element method. Eng. Anal. Bound. Elem. **30**, 441–418 (2006)
4. M. Tezer-Sezgin, S. Han-Aydın, BEM solution of MHD flow in a pipe coupled with magnetic induction of exterior region. Computing **95**(1), 751–770 (2013)
5. M. Tezer-Sezgin, S. Han-Aydın, DRBEM solution of MHD pipe flow in a conducting medium. J. Comput. Appl. Math. **259**, 720–729 (2014)
6. C. Bozkaya, M. Tezer-Sezgin, A direct BEM solution to MHD flow in electrodynamically coupled rectangular channels. Comput. Fluids **66**, 177–182 (2012)
7. S. Han-Aydın, A.I. Neslitürk, M. Tezer-Sezgin, Two-level finite element method with a stabilizing subgrid for the incompressible MHD equations. Int. J. Numer. Methods Fluids **62**, 188–210 (2010)
8. M. Tezer-Sezgin, C. Bozkaya, Ö. Türk, BEM and FEM based numerical simulations for biomagnetic fluid. Eng. Anal. Bound. Elem. **37**(9), 1127–1135 (2013)
9. E.E. Tzirtzilakis, V.D. Sakalis, N.G. Kafoussias, P.M. Hatzikonstantinou, Biomagnetic fluid flow in a 3D rectangular duct. Int. J. Numer. Methods Fluids **44**, 1279–1298 (2004)
10. E.E. Tzirtzilakis, A mathematical model for blood flow in magnetic field. Phys. Fluids **17**, 077103 (2005)
11. E.E. Tzirtzilakis, M.A. Xenos, Biomagnetic fluid flow in a driven cavity. Meccanica **48**, 187–200 (2013)
12. U. Müller, L. Bühler, *Magnetofluiddynamics in Channels and Containers* (Springer, Berlin/New York, 2001)
13. W. Layton, H. Tran, C. Trenchea, *Numerical analysis of two partitioned methods for uncoupling evalutionary MHD flows*. Numer. Methods Partial Differ. Eq. **30**, 108301102 (2014)
14. P.W. Partridge, C.A. Brebbia, L.C. Wrobel, *The Dual Reciprocity Boundary Element Method* (Computational Mechanics Publications, Southampton/Boston, 1992)

DRBEM Solution of the Double Diffusive Convective Flow

Canan Bozkaya and Münevver Tezer-Sezgin

Abstract A numerical investigation of unsteady, two-dimensional double diffusive convection flow through a lid-driven square enclosure is carried on. The left and bottom walls of the enclosure are either uniformly or non-uniformly heated and concentrated, while the right vertical wall is maintained at a constant cold temperature. The top wall is insulated and it moves to the right with a constant velocity. The numerical solution of the coupled nonlinear differential equations is based on the use of dual reciprocity boundary element method (DRBEM) in spatial discretization and an unconditionally stable backward implicit finite difference scheme for the time integration. Due to the coupling and the nonlinearity, an iterative process is employed between the equations. The boundary only nature of the DRBEM and the use of the fundamental solution of Laplace equation make the solution process computationally easier and less expensive compared to other domain discretization methods. The study focuses on the effects of uniform and non-uniform heating and concentration of the walls for various values of physical parameters on the double-diffusive convection in terms of streamlines, isotherms and isoconcentration lines.

1 Introduction

Double-diffusive convection describes a form of convection driven by two different density gradients which have different rates of diffusion. In this sense, the double-diffusive convection generally refers to a fluid flow generated by buoyancy effects due to both temperature and solute concentration gradients. This type of flow is encountered in many engineering and geophysical applications, such as nuclear reactors, solar ponds, geothermal reservoirs, solar collectors, crystal growth in liquids, electronic cooling and chemical processing equipments. Thus, a clear understanding of the interaction between the thermal and mass or solute concentration buoyancy forces is necessary in order to control these processes.

C. Bozkaya (✉) • M. Tezer-Sezgin
Department of Mathematics, Middle East Technical University, 06800, Ankara, Turkey
e-mail: bcanan@metu.edu.tr; munt@metu.edu.tr

B. Karasözen et al. (eds.), *Numerical Mathematics and Advanced Applications ENUMATH 2015*, Lecture Notes in Computational Science and Engineering 112, DOI 10.1007/978-3-319-39929-4_2

In the literature, the double-diffusive heat and mass transfer problems are studied mostly for square or rectangular geometries with different thermal and solute boundary conditions by using several experimental and numerical techniques. Lee et al. [1] studied experimentally the steady natural convection of salt-water solution due to horizontal temperature and concentration gradients. Cooper et al. [2] carried experiments to see the effect of buoyancy ratio R_p on the development of double-diffusive finger convection in a Hele-Shaw cell. They observed that, for low R_p fingers are rapidly developed and merge with adjacent fingers, while at higher R_p fingers are slower to evolve and do not interact as dynamically as in the lower R_p system. On the other hand, the unsteady double-diffusive convection in a square cavity was solved by Zhan et al. [3] to investigate the advantage of a hybrid method over commercial CFD codes. A finite volume approach was employed for the solution of double-diffusion flow in a cavity in [4, 5]. The effect of uniform and non-uniform heating of the walls on the double-diffusive convection in a lid-driven square cavity was analyzed by using a staggered grid finite difference method by Mahapatra et al. [6]. Alsoy et al. [7] solved the mixed convective in a lid-driven cavity and through channels with backward-facing step by the use of DRBEM.

It is seemed that, to the best of our knowledge, the double-diffusive convection in a lid-driven cavity with uniformly and non-uniformly heated and concentrated walls has not been solved by using the DRBEM which gives the solution at a considerably low computational expense due to its boundary-only nature. In the present study, we undertake this task varying the thermal Rayleigh number Ra_T and the buoyancy ratio R_p. A comprehensive study of the heat and mass transfer in terms of the flow field, temperature and concentration distribution is given in details.

2 Governing Equations

The unsteady, laminar, two-dimensional double-diffusive convection flow of an incompressible, Newtonian and viscous fluid in a lid-driven square cavity is considered. The thermo-physical properties of the fluid are assumed to be constant except the density variation in the buoyancy force, which is approximated according to the Boussinesq approximation. Thus, the non-dimensional unsteady double-diffusive convection equations in the stream function-vorticity-temperature form are written as [6]:

$$\nabla^2 \psi = -\omega \tag{1}$$

$$Pr\nabla^2 \omega = \frac{\partial \omega}{\partial t} + \mathbf{u}.\nabla\omega - PrRa_T \left(\frac{\partial \theta}{\partial x} + R_p \frac{\partial S}{\partial x} \right) \tag{2}$$

$$\nabla^2 \theta = \frac{\partial \theta}{\partial t} + \mathbf{u}.\nabla\theta \tag{3}$$

$$\frac{1}{Le}\nabla^2 S = \frac{\partial S}{\partial t} + \mathbf{u}.\nabla S \tag{4}$$

where

$$Ra_T = \frac{g\beta_T(T_h - T_c)\ell^3}{\nu\alpha}, \quad Ra_S = \frac{g\beta_S(C_h - C_c)\ell^3}{\nu D}, \quad R_p = \frac{Ra_S}{Ra_T Le},$$

$$Pr = \frac{\nu}{\alpha}, \quad Le = \frac{\alpha}{D}.$$

Here, $\mathbf{u} = (u, v)$, ψ, w, θ, S are the velocity field, stream function, vorticity, temperature, concentration, and Pr and Le are the Prandtl number and Lewis number, respectively. The physical parameters g, α, D, ν and l given in the definitions of the thermal Rayleigh number (Ra_T) and the solutal Rayleigh number (Ra_S) are respectively the gravitational acceleration, thermal diffusivity, molecular (mass) diffusivity, kinematic viscosity and side length of the cavity. The temperatures and the concentrations at the hot and cold walls are denoted by T_h, T_c and C_h, C_c, respectively. The buoyancy ratio (R_p) is a ratio of fluid density contributions by the two solutes and defines the degree of system disequilibrium.

The corresponding dimensionless boundary conditions when $t > 0$ are shown in Fig. 1, while all unknowns are initially (at $t = 0$) taken as zero (i.e. $\psi = w = \theta = S = 0,\ 0 \le x, y \le \ell$). The thermally insulated top wall of the cavity moves to the right with a constant velocity ($\psi_y = 1$, $\psi_x = 0$), while the no-slip boundary condition is employed to the remaining walls ($\psi_x = \psi_y = 0$). Further, the bottom and left walls of the cavity are either uniformly ($\theta = S = 1$) or non-uniformly ($\theta = S = \sin \pi x$ at $y = 0$ and $\theta = S = \sin \pi y$ at $x = 0$) heated and concentrated, while the right wall is kept cold. On the other hand, the unknown boundary vorticity

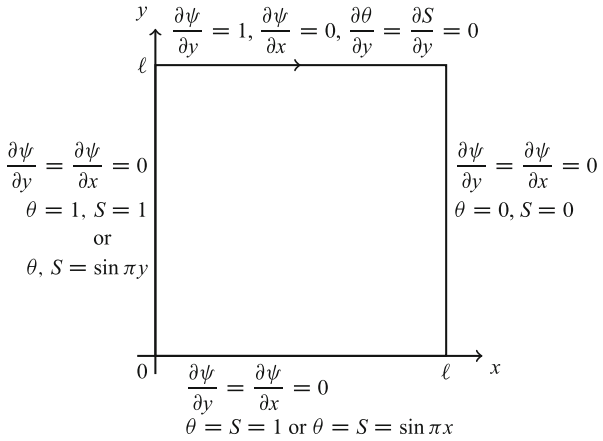

Fig. 1 Schematic diagram of the problem with boundary conditions

values will be obtained from the stream function equation $\Delta\psi = -w$ by using a radial basis function approximation.

3 Application of the DRBEM

The governing Eqs. (1), (2), (3), and (4) are transformed into the equivalent boundary integral equations by using DRBEM with the fundamental solution of the Laplace equation, $u^* = -\ln(r)/2\pi$, and by treating all the terms on the right hand side as inhomogeneity. An approximation for these inhomogeneous terms is

$$b \approx \sum_{j=1}^{N+L} \alpha_j f_j = \sum_{j=1}^{N+L} \alpha_j \nabla^2 \hat{u}_j$$

as proposed in [8]. Here, N and L are the numbers of boundary and interior nodes, α_j are sets of initially unknown coefficients, and f_j are approximating radial basis functions linked to particular solutions $\hat{u}_j$ with $\nabla^2 \hat{u}_j = f_j$. The radial basis functions f_j are chosen as linear polynomials (i.e. $f_j = 1 + r_j$), where r_j is the distance between the source and field points.

By the use of Divergence theorem for the Laplacian terms on both sides of the equation, domain integrals are transformed into the boundary integrals. Then, constant elements are used for the discretization of the boundary, which results in the following DRBEM matrix-vector form of Eqs. (1), (2), (3), and (4)

$$H\psi - G\psi_q = C\{-\omega\}\,, \tag{5}$$

$$H\omega - G\omega_q = C\left\{\frac{1}{Pr}\left[\frac{\partial\omega}{\partial t} + \mathbf{u}.\nabla\omega - PrRa_T\left(\frac{\partial\theta}{\partial x} + R_p\frac{\partial S}{\partial x}\right)\right]\right\} \tag{6}$$

$$H\theta - G\theta_q = C\left\{\frac{\partial\theta}{\partial t} + \mathbf{u}.\nabla\theta\right\} \tag{7}$$

$$HS - GS_q = C\left\{Le\left(\frac{\partial S}{\partial t} + \mathbf{u}.\nabla S\right)\right\} \tag{8}$$

where $\psi_q = \partial\psi/\partial n$, $\omega_q = \partial\omega/\partial n$, $\theta_q = \partial\theta/\partial n$, $S_q = \partial S/\partial n$, $q^* = \partial u^*/\partial n$ and H and G are the usual DRBEM matrices. The matrix $C = (H\hat{U} - G\hat{Q})F^{-1}$ in which the matrices $\hat{U}$ and $\hat{Q}$ are constructed by taking each of the vectors $\hat{u}_j$ and $\hat{q}_j$ as columns, respectively.

The unconditionally stable backward difference integration scheme defined by

$$\frac{\partial u}{\partial t}\Big|^{n+1} = \frac{u^{n+1} - u^n}{\Delta t}$$

is used for the time integration. Here n indicates the time level. Thus, the time discretized form of DRBEM system of algebraic equations for the stream function, vorticity, temperature and concentration takes the form

$$H\psi^{n+1} - G\psi_q^{n+1} = -Cw^n \,, \tag{9}$$

$$(H - \frac{1}{Pr\Delta t}C - \frac{1}{Pr}CK)\omega^{n+1} - G\omega_q^{n+1} = -\frac{1}{Pr\Delta t}C\omega^n - Ra_T CD_x(\theta^n + R_p S^n) \tag{10}$$

$$(H - \frac{1}{\Delta t}C - CK)\theta^{n+1} - G\theta_q^{n+1} = -\frac{1}{\Delta t}C\theta^n \tag{11}$$

$$(H - \frac{Le}{\Delta t}C - LeCK)S^{n+1} - GS_q^{n+1} = -\frac{Le}{\Delta t}CS^n \tag{12}$$

where $K = u^{n+1}D_x + v^{n+1}D_y$, $D_x = \dfrac{\partial F}{\partial x}F^{-1}$ and $D_y = \dfrac{\partial F}{\partial y}F^{-1}$. The resulting system of coupled Eqs. (9), (10), (11), and (12) is solved iteratively with initial estimates of ω, θ and S. In each time level, the required space derivatives of the unknowns ψ, ω, θ and S are obtained by using coordinate matrix F as $\dfrac{\partial \Phi}{\partial x} = \dfrac{\partial F}{\partial x}F^{-1}\Phi$, $\dfrac{\partial \Phi}{\partial y} = \dfrac{\partial F}{\partial y}F^{-1}\Phi$, where Φ represents the unknowns ψ, ω, S or θ. The iterative process is terminated when a preassigned tolerance (e.g. 10^{-5}) is reached between two successive iterations.

4 Numerical Results

The unsteady double-diffusive convection in a lid-driven square cavity with uniformly and non-uniformly heated and concentrated walls is analyzed by using coupling of the DRBEM with constant elements in space with an unconditionally unstable backward difference scheme in time. The domain of problem is determined by taking the side length of the cavity $\ell = 1$. The boundary of the cavity is discretized by using maximum $N = 90$ constant boundary elements. Numerical calculations are carried out for various values of Rayleigh number ($Ra_T = 10^3, 10^5$) and buoyancy ratio ($-50 \le R_p \le 50$) by fixing $Pr = 0.7$ and $Le = 2$.

Figure 2 displays the effect of the Rayleigh number on the flow field, temperature and concentration at $R_p = 1$ when the bottom and left walls of the cavity are (a) uniformly (b) non-uniformly heated and concentrated. A roll with clockwise rotation is formed inside the cavity since the fluid rises up and flows down, respectively, along the hot left and cold right vertical walls. As Ra_T increases from 10^3 to 10^5, the values of stream function increase in magnitude and the flow becomes stagnant in the core of the cavity in both uniform and non-uniform cases. On the other hand, the isotherms and isoconcentration lines are dispersed in the entire cavity

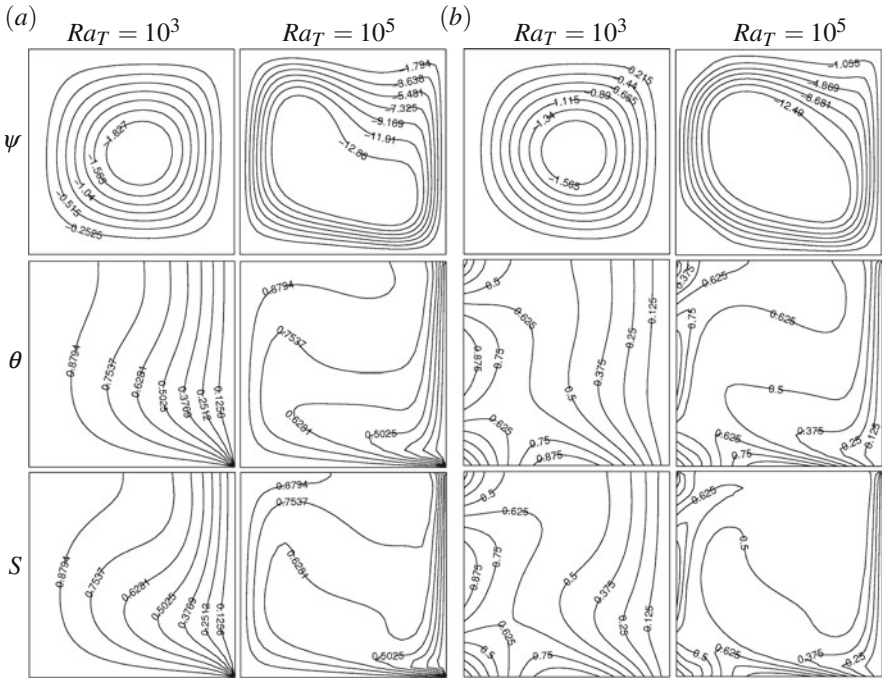

Fig. 2 Effect of the Rayleigh number Ra_T on the flow field, temperature and concentration at $R_p = 1$: *bottom* and *left walls* are (**a**) uniformly (**b**) non-uniformly heated and concentrated

at $Ra_T = 10^3$, however, lines are concentrated along the cold left vertical wall with an increase in Ra_T to 10^5 in both cases.

Effect of the buoyancy ratio R_p on the flow field, temperature and concentration at $Ra_T = 10^3$ is shown in Fig. 3 when the bottom and left walls are (a) uniformly and (b) non-uniformly heated and concentrated. In both uniform and non-uniform cases, the strength of the flow circulation decreases with a decrease in buoyancy ratio from $R_p = 50$ to $R_p = 1$ (see Fig. 2), while the stream function values increase in magnitude with a further decrease from $R_p = 1$ to $R_p = -50$. At $R_p = 50$, the contours of θ and S are mainly concentrated near the cold vertical wall and they are dispersed towards to right wall at $R_p = 1$ (see Fig. 2) in both cases. However, when $R_p = -50$, the isotherms and the isoconcentration lines are concentrated near the lower and upper half of the cold and hot vertical walls, respectively. They are almost parallel to horizontal wall in the middle part of cavity at $R_p = -50$, indicating that most of the heat transfer is carried out by heat conduction. This is due to an increase in thermal boundary layer thickness. As R_p increases boundary layer becomes thinner. This change in flow structure significantly influences the concentration field, which builds up a vertical stratification of enclosure in both uniform and non-uniform cases. The uniform heating of bottom and left walls cause a finite discontinuity for temperature distribution at one edge of bottom wall